I&EC research
Industrial & Engineering Chemistry Research

Article

Cite This: Ind. Eng. Chem. Res. 2017, 56, 14053-14059

pubs.acs.org/IECR

Facile Preparation of α-Calcium Sulfate Hemihydrate with Low Aspect Ratio Using High-Gravity Reactive Precipitation Combined with a Salt Solution Method at Atmospheric Pressure

Yong-Qing Zhang,[‡] Dan Wang,[‡,§] Liang-Liang Zhang,*[,§] Yuan Le,[‡,§] Jie-Xin Wang,*[,†,‡,§] and Jian-Feng Chen[†,‡,§]

[†]Beijing Advanced Innovation Center for Soft Matter Science and Engineering, Beijing University of Chemical Technology, Beijing 100029, People's Republic of China

[‡]State Key Laboratory of Organic−Inorganic Composites, Beijing University of Chemical Technology, Beijing 100029, People's Republic of China

[§]Research Center of the Ministry of Education for High Gravity Engineering and Technology, Beijing University of Chemical Technology, Beijing 100029, People's Republic of China

Supporting Information

ABSTRACT: As one of the important bone regeneration materials, α-calcium sulfate hemihydrate (α-CSH) has attracted widespread attention. In this study, a facile method was developed to prepare α-CSH with low aspect ratio via high-gravity continuously reactive precipitation of a calcium sulfate dihydrate (CSD) precursor, using ethanol as a morphology modifier in a rotating packed bed (RPB) reactor, combined with $CaCl_2$ salt solution method under atmospheric pressure with the addition of citric acid with a low concentration (0.06 wt %). The precipitation time of CSD powders in the RPB was dramatically shortened from 30 min to 1 s, and the precursor exhibited more regular short rod shapes and much smaller size, compared to that obtained in a conventional stirring tank reactor (STR). Furthermore, calcium sulfate bone materials with high stability and good mechanical property were prepared by mixing α-CSH and normal saline with a liquid−solid ratio of 0.6. The RPB products had a higher compressive strength (2−3 times) than the STR counterpart.

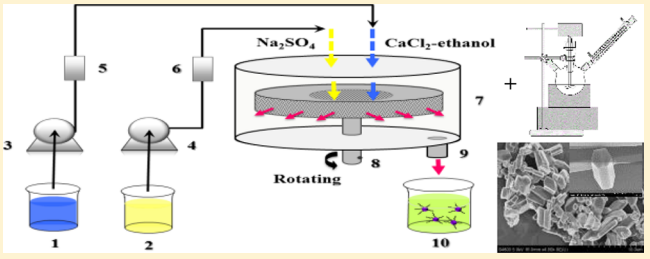

1. INTRODUCTION

Calcium sulfate (CS), which is a very important industrial material, usually exists in three forms, including anhydrite ($CaSO_4$, CSA), hemihydrate ($CaSO_4{\cdot}0.5H_2O$, CSH (α-CSH and β-CSH)), and dihydrate ($CaSO_4{\cdot}2H_2O$, CSD).[1−3] Among them, much attention has been given to α-CSH, because it has gained more applications in orthopedic and dental fields, including bone cement, bone graft substitutes, and scaffolds for delivering growth factors for osseous regeneration.[4−6] The performance of α-CSH is closely associated with the size and the morphology of crystals. It is reported that α-CSH crystals with lower aspect ratio are preferable for use in bone cement, because they are easier to inject and have better mechanical properties.[7,8]

Many strategies have been utilized to prepare α-CSH via the direct conversion of flue gas desulfurization gypsum or calcium sulfite hemihydrate,[9−11] reverse microemulsion,[8,12] ultrasound/microwave-assisted method,[13,14] and a commonly used two-stage process, including the formation of CSD from the reactions between sulfuric acid and lime or soluble sulfate and calcium salt, followed by the conversion to α-CSH via dehydration process.[15−19] In the two-stage process, the morphology and the size of the CSD precursor have significant effects on the final α-CSH product, thereby affecting the medical properties and the strength of calcium sulfate-based materials.[20] For the reactive precipitation process between soluble sulfate and calcium salt, it is crucial to achieve a homogeneous supersaturation environment quickly for the nucleation and growth of CSD particles, which is very beneficial to form smaller particle sizes and regular shapes.

A rotating packed bed (RPB), known as Higee apparatus, can generate a high-gravity environment to strongly intensify the micromixing and mass-transfer processes, thereby providing even reaction surroundings.[21−23] It is believed to be a promising reactor for the continuous production of many inorganic and organic ultrafine particles or nanoparticles.[24−29] Compared to a conventional stirred tank reactor (STR), RPB has many advantages, such as smaller particle size with narrower size distribution, shorter reaction time, easier industrialization, etc.

Received: August 13, 2017
Revised: November 2, 2017
Accepted: November 6, 2017
Published: November 7, 2017

DOI: 10.1021/acs.iecr.7b03356
Ind. Eng. Chem. Res. 2017, 56, 14053−14059

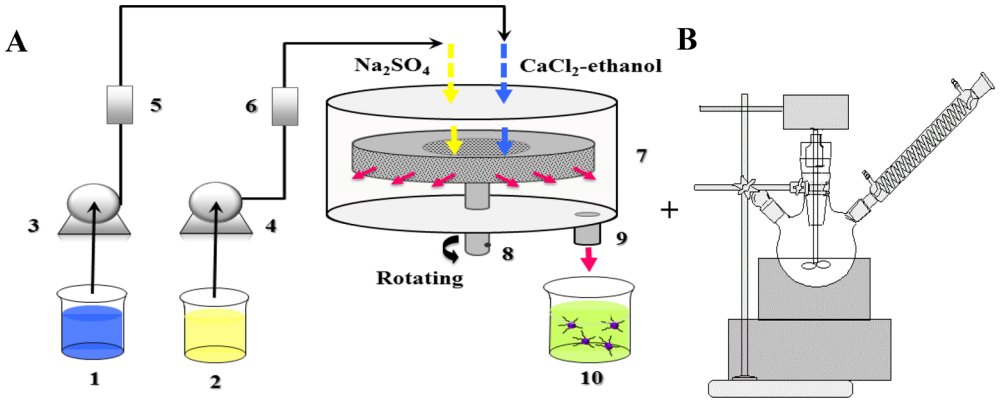

Figure 1. (A) Schematic diagram of experimental setup for high-gravity reactive precipitation process (legend: (1) $CaCl_2$ solution tank; (2) Na_2SO_4 solution tank; (3, 4) pumps; (5, 6) flow meters; (7) RPB reactor; (8) motor; (9) liquid outlet; and (10) outlet tank). (B) Diagram of the device used for the salt solution method at atmospheric pressure.

In this study, a combined route of high-gravity reactive precipitation and salt solution method under atmospheric pressure was first employed to prepare α-CSH with a low aspect ratio. First, CSD precursor was facilely prepared through the reaction between Na_2SO_4 and $CaCl_2$ in an ethanol/water mixture in the RPB reactor. Ethanol was used as a morphology modifier to control the final morphology of CSD crystals. The $CaCl_2$ salt solution method at atmospheric pressure with the key addition of citric acid with a low concentration, based on a dissolution−crystallization mechanism, was then used to dehydrate the as-prepared CSD precusor to obtain the final α-CSH product. In addition, a batch STR was also used to prepare α-CSH for comparison. Furthermore, calcium sulfate bone materials were fabricated by mixing as-prepared α-CSH with normal saline, and the corresponding mechanical properties were also evaluated.

2. EXPERIMENTAL SECTION

2.1. Materials and Setup. Analytical reagent (AR)-grade $CaCl_2$, Na_2SO_4, citric acid, and anhydrous ethanol were purchased from the Beijing Tongguang Fine Chemicals Company. Deionized water was used throughout the study. The experimental setup for the preparation of α-CSH is schematically shown in Figure 1. The key apparatus of the entire procedure was the RPB reactor, consisting of a packed rotator, a fixed casing, two liquid inlets, and a suspension outlet. The rotator had an inner diameter of 36 mm, an outer diameter of 84 mm, and the axial length of 40 mm. The bed was filled with stainless wire meshes with a porosity of 0.9 and a surface area of 850 m^2/m^3. The packing consists of 20 layers. The rotator was installed inside the fixed casing and rotates at an adjustable speed. For more details about the struture of the RPB reactor, the reader is referred to our previously published papers.[22,24,25]

2.2. Preparation of α-CSH. In a typical procedure, 250 mL of 1 mol/L $CaCl_2$ mixed solution with different ethanol−water volume ratios (0:3, 1:3, 2:3, 1:1, and 4:3) and 250 mL of 1 mol/L Na_2SO_4 solution were first prepared. Subsequently, both solutions with a flow rate of 0.5 L/min were simultaneously pumped into the RPB reactor with a rotating speed of 2500 rpm at room temperature. The contact and reaction times of the reactants in the RPB reactor were ∼1 s. The precipitated CSD precursor collected from the outlet of the RPB was filtered, and then washed (three times with DI water and one time with anhydrous ethanol). The filter cake was dried at 50 °C overnight to obtain CSD powder. The conversion from CSD precursor to α-CSH product was conducted in a three-neck flask that was equipped with a condenser for vapor reflux. A quantity of 150 mL of 25 wt % $CaCl_2$ solution with 0.06 wt % citric acid additive and an initial pH value of ∼4.4 was prepared, and then added into the three-neck flask with a vigorous stirring in an oil bath at 95 °C. After 30 min, CSD precursor was further added into the flask with a CSD/water mass ratio of 1:20, and the mixture was allowed to react for 4 h. When the reaction was finished, the slurry was immediately filtered and rinsed three times with hot water (90−95 °C) to prevent the hydration process. Finally, the obtained filter cake was immersed in ethanol for 1 min, filtered again, and then dried at 100 °C for 4 h to achieve the final α-CSH product.

As a comparison, CSD precursor was also similarly prepared in a conventional STR. Briefly, 250 mL of 1 mol/L $CaCl_2$ aqueous solution was rapidly added into 250 mL of 1 mol/L Na_2SO_4 solution under vigorous stirring. After the reaction process lasted for 30 min, the suspension was filtered, and then washed (three times with deionized (DI) water and one time with anhydrous ethanol). The following salt solution treatment at atmospheric pressure was performed in the above-mentioned same way to obtain the final α-CSH product.

2.3. Preparation of Calcium Sulfate Bone Materials. Calcium sulfate bone materials were fabricated by mixing the above as-prepared α-CSH and normal saline. Briefly, α-CSH powder was added into the normal saline to form an adhesive paste with different liquid−solid ratios of 0.2−1.8. After uniformly stirring, the cement slurry was filled into a cylinder mold with a radius of 9 mm and a height of 14 mm to prepare the sample for the measurement of mechanical properties. Finally, the sample was solidified at 37 °C in an oven for 48 h.

2.4. Characterization. The morphology and the size of the samples were characterized at an accelerating voltage of 10 kV with a scanning electron microscopy (SEM) system (Model JEOL-7800, JEOL, Japan). X-ray diffraction (XRD) measurements were performed by a diffractometer (Model D8 Avance, Bruker, Germany) equipped with Cu Kα radiation, using an accelerating voltage of 40 kV and a current of 40 mA. The scanning range was 5°−50°, and the scanning rate was 8°/min, with a step size of 0.01°. A Fourier transform infrared (FT-IR) spectrum of the sample was recorded in the wavenumber range of 500−4000 cm^{-1}, using a spectrometer (Model Nicolet 6700, Nicolet Instrument Co., USA). Thermogravimetric analysis (TGA) was carried out on a thermogravimetric/differential

DOI: 10.1021/acs.iecr.7b03356
Ind. Eng. Chem. Res. 2017, 56, 14053−14059

thermal analyzer (Model STA-449C, Netzsch, Germany) from 20 °C to 600 °C, using a heating rate of 10 °C/min in an Ar atmosphere. The compressive strength of the sample was measured by a universal material testing machine (Model XM-SFC001, China), using a loading speed of 0.5 mm/min. Each sample was analyzed in triplicate. The average value was obtained.

3. RESULTS AND DISCUSSION

Figure 2 shows SEM images of CSD precursors prepared with no addition of ethanol in the STR (Figure 2A) and in the RPB reactor with different ethanol/water volume ratios (Figures 2B–F). There were still no obvious white precipitates in the traditional STR after the reaction was performed for 20 s. However, a large amount of precipitate was immediately created after both reactants had a fast contact of ~1 s in the RPB reactor, indicating the huge improvement of precipitation efficiency. After 30 min, CSD precursors produced in the STR had an irregular thick platelike morphology, with lengths in the range of 20–40 μm and a width of 8–10 μm (Figure 2A). Correspondingly, the instantaneously formed CSD particles with no addition of ethanol in the RPB reactor had relatively uniform rodlike shapes and a much smaller size, with an average length of 6–15 μm and a width of 1–3 μm (Figure 2B). The above results are mainly ascribed to the fact that the fluids passing through the porous packing in the high-speed rotating state were intensively split into tiny droplets, thereby greatly increasing the contact interfacial area and significantly intensifying the micromixing of the fluid elements.[27,30] This is very beneficial to the rapid formation of a homogeneous nucleation and reaction environment for preparing small particles with narrow size distribution. In addition, by comparing Figure 2B and Figures 2C–F, it could be observed that the addition of ethanol in the RPB could further effectively decrease the size of the CSD crystals and generate a more uniform morphology. In particular, when the ethanol/water volume ratio was 1:3, the length and the width of CSD particles obviously decreased to 0.6–3 μm and 0.3–0.8 μm, reaching a lower aspect ratio of 2–4. However, as the ethanol/water volume ratio increased from 1:3 to 4:3, the width of particles experienced only a slight change, but the length of particles and the corresponding aspect ratio markedly increased to 5–15 μm and 8–18, respectively (see Table S1 in the Supporting Information). Such a phenomenon is complicated, but it could be reasonably explained in terms of the following possible mechanism. On the one hand, the addition of ethanol changes the chemical properties of the solvent in the supersaturation of CSD, such as the dielectric constant of the medium, ion interattraction, and the solute–solvent interaction, as a result of the solubility difference. This will lead to greater supersaturation, which is beneficial to the formation of smaller particles.[3] When the ethanol/water volume ratio is further increased to over 1:3, this action is weakened. On the other hand, ethanol can modify the surface energies of specific crystal planes. It is well-known that Ca^{2+} is coordinated by six sulfate O atoms and two water molecules along the *c*-axis in CSD, preferentially leading to anisotropic growth along the *c*-axis direction.[3] Therefore, CSD particles with the obviously increased length and higher aspect ratio were thus formed, from the increase of ethanol concentration resulting from the increased ethanol/water volume ratio. Since the objective of this study was to prepare α-CSH with smaller size and lower aspect ratio, the ethanol/water volume ratio was determined as 1:3 in the subsequent investigation.

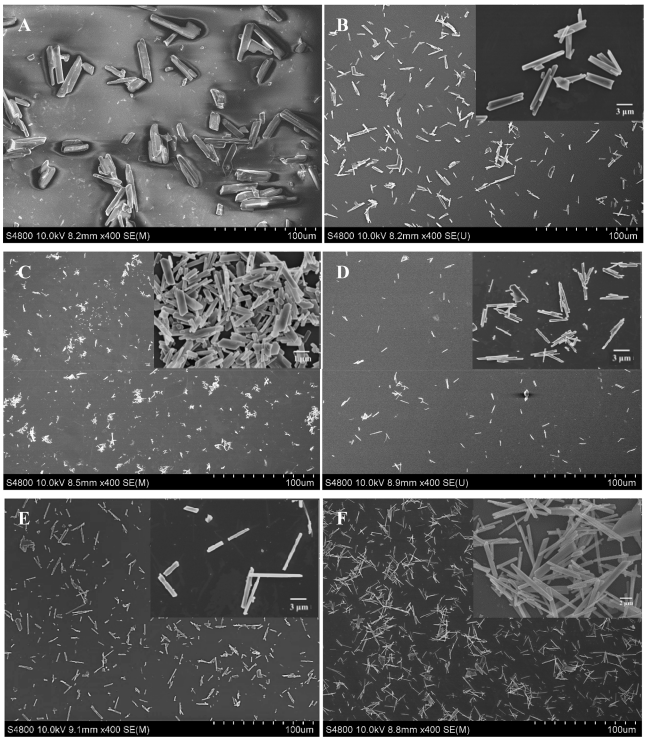

Figure 2. SEM images of CSD precursors prepared with no addition of ethanol (A) in the STR and (B–F) in the RPB reactor with different ethanol/water volume ratios (0:3 panel (B), 1:3 panel (C), 2:3 panel (D), 1:1 panel (E), and 4:3 panel (F)).

Figure 3 gives XRD patterns of CSD precursors prepared under the optimum conditions with different reactive precipitation processes. All peaks of three samples were indexed corresponding to standard CSD (Joint Committee on Powder Diffraction Standards (JCPDS) File No. 33-0311) with the monoclinic structure, indicating a fully crystallized CSD phase. However, the CSD precursor prepared in the RPB had significantly weakened diffraction peaks, compared to the CSD precursor prepared in the STR, especially in the (020), (021), (040), and (041) lattice planes, which are mainly ascribed to smaller particle size. Furthermore, the CSD

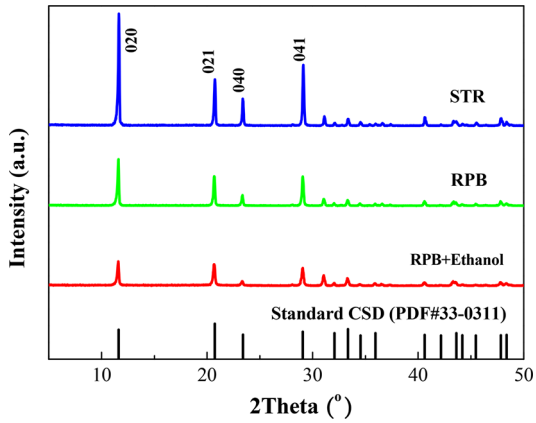

Figure 3. XRD patterns of CSD precursors prepared under the optimum conditions with different reactive precipitation processes.

DOI: 10.1021/acs.iecr.7b03356
Ind. Eng. Chem. Res. 2017, 56, 14053–14059

precursor that was prepared with the addition of ethanol in the RPB had further weakened diffraction peaks, because of CSD precursors with smaller size and lower aspect ratio. The above results were in good accord with the SEM images in Figures 2A–C.

Figure 4 shows typical SEM images of α-CSH products prepared under the optimum conditions using different reactive

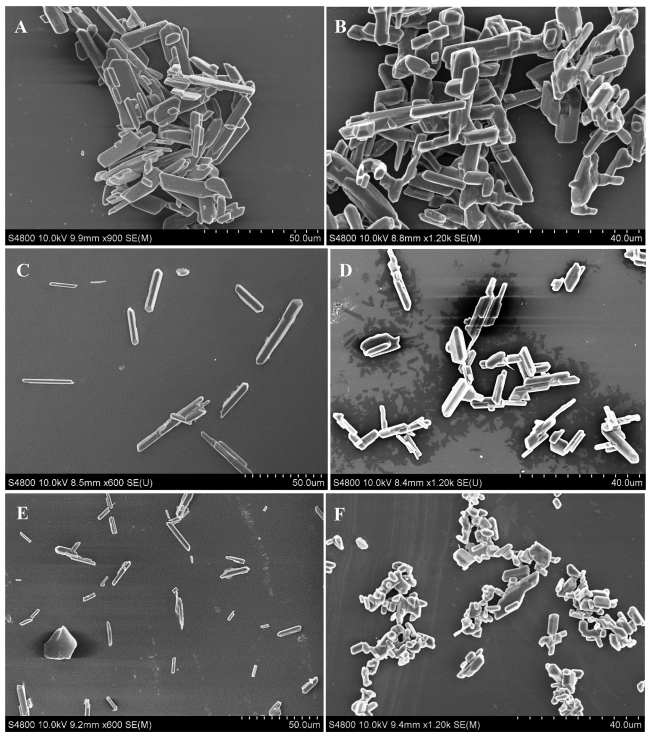

Figure 4. SEM images of α-CSH products prepared under the optimum conditions using different reactive precipitation processes ((A, B) STR, (C, D) RPB, and (E, F) RPB + ethanol) combined with a salt solution method at atmospheric pressure (panels (A), (C), and (E) show results with no addition of citric acid; panels (B), (D), (F) show results with the addition of citric acid).

precipitation processes combined with a salt solution method at atmospheric pressure without and with 0.06 wt % citric acid additive. In the $CaCl_2$ solution without citric acid additive (Figure 4A), the resultant α-CSH product transformed from the CSD precipitate obtained in the STR had an obvious thin platelike morphology with a length of 20–30 μm and a width of 10–15 μm. However, the as-prepared α-CSH products transformed from the CSD precipitate obtained in the RPB had a rodlike morphology (see Figures 4C and 4E). Moreover, because of the addition of ethanol in the precipitation process, the corresponding α-CSH product had a smaller particle size, with a length of 10–15 μm and a width of 2–4 μm (see Figure 4E), as compared to that shown in Figure 4C (which had a length of 15–35 μm and a width of 3–7 μm). This completely indicated that the morphology and the size of CSD precursor had a significant effect on the final α-CSH product. Furthermore, because of the addition of citric acid, there was a shape change for the STR product from platelike to rodlike, and a big reduction of aspect ratio of rodlike particles for the RPB products, which is very beneficial to the achievement of better strength properties.[7,8] Obviously, citric acid plays a very important role in controlling the morphology and decreasing the aspect ratio in the salt solution process, despite the addition of such a low concentration (0.06 wt %). It is reasonable to deduce that the interaction between citric acid and α-CSH crystallites inhibits the crystal growth. Citric acid as a crystal modifier can be selectively adsorbed on specific crystal planes to alter their surface energy. Therefore, the growth rate of planes along the *c*-axis slows, and the morphology of α-CSH crystals changes from long and thin prisms to short and thick prisms, as indicated by the contrast between the dimensions of the products without and with citric acid (Figures 4A, 4C, and 4E and Figures 4B, 4D, and 4F). This result was similar to the action of other reported additives, such as surfactants or succinic acid.[31–33]

Figure 5 presents typical SEM images, XRD pattern, an FTIR spectrum, and TG-DSC curves of α-CSH product prepared under optimum conditions. Clearly, as shown in Figure 5A, the as-prepared α-CSH particles had a short, well-crystallized hexagon-prism shape, a length of 1–6 μm, a width of 1–2 μm, and an aspect ratio of 1–3. The XRD pattern indicated that the product matched well with the standard pattern of α-CSH (JCPDS File No. 23-0128). The FTIR spectrum in Figure 5C further confirmed the α-CSH, by the evidence of its characteristic peaks emerging at 3610.58 and 3554.65 cm^{-1} (vibration of H_2O groups), 1622.06 cm^{-1}, 1153.38 cm^{-1}, 1093.59 cm^{-1}, 657.70 cm^{-1}, 599.83 cm^{-1} (SO_4^{2-} stretching). Citric acid could not be detected, because of of its very tiny amount of addition. TG-DSC curves in Figure 5D showed a sharp endothermic peak at 150.51 °C and a corresponding weight loss of 6.18% in the temperature range of 95–150 °C, which was ascribed to the removal of 0.5 crystalline water molecules from α-CSH to CSA, which was almost consistent with the theoretical value of 6.21%, thereby proving the presence of pure α-CSH.

After α-CSH product was achieved, calcium sulfate bone material was further prepared by mixing α-CSH and normal saline. The as-prepared calcium sulfate bone material still remained unchanged and was never dispersed after immersion in normal saline for 60 d (see Figure S1 in the Supporting Information), well demonstrating its high stability. Figure 6 shows the effect of liquid–solid ratio on the compressive strength of calcium sulfate bone material, and the compressive strengths of calcium sulfate bone materials prepared with different α-CSH samples. As shown in Figure 6A, it could be clearly found that the compressive strength first increased and then decreased with the increased liquid–solid ratio from 0.2 to 1.8. At a liquid–solid ratio of 0.6, the highest compressive strength (18.37 MPa) was observed. This is because the mixing between α-CSH and normal saline is a hydration process. It is exothermic and can generate microbubbles. Therefore, porosity forms in the calcium sulfate bone materials. Since the liquid–solid ratio directly determines the porosity that is formed, a higher liquid–solid ratio leads to more microbubbles and higher porosity, thereby causing a decrease in the corresponding compressive strength. Therefore, the liquid–solid ratio should be properly reduced. However, with a liquid–solid ratio that is too low, it is difficult to make α-CSH powder completely wetting, which creates a heterogeneous porosity, thereby decreasing the compressive strength. Therefore, the suitable liquid–solid ratio was determined as 0.6. Figure 6B compares the compressive strengths of calcium sulfate bone materials prepared with different α-CSH samples based on the optimal liquid–solid ratio. Obviously, the product from the RPB had a compressive strength of 12.17 MPa, which was almost twice as much as that (6.46 MPa) of the counterpart from the STR,

DOI: 10.1021/acs.iecr.7b03356
Ind. Eng. Chem. Res. 2017, 56, 14053–14059

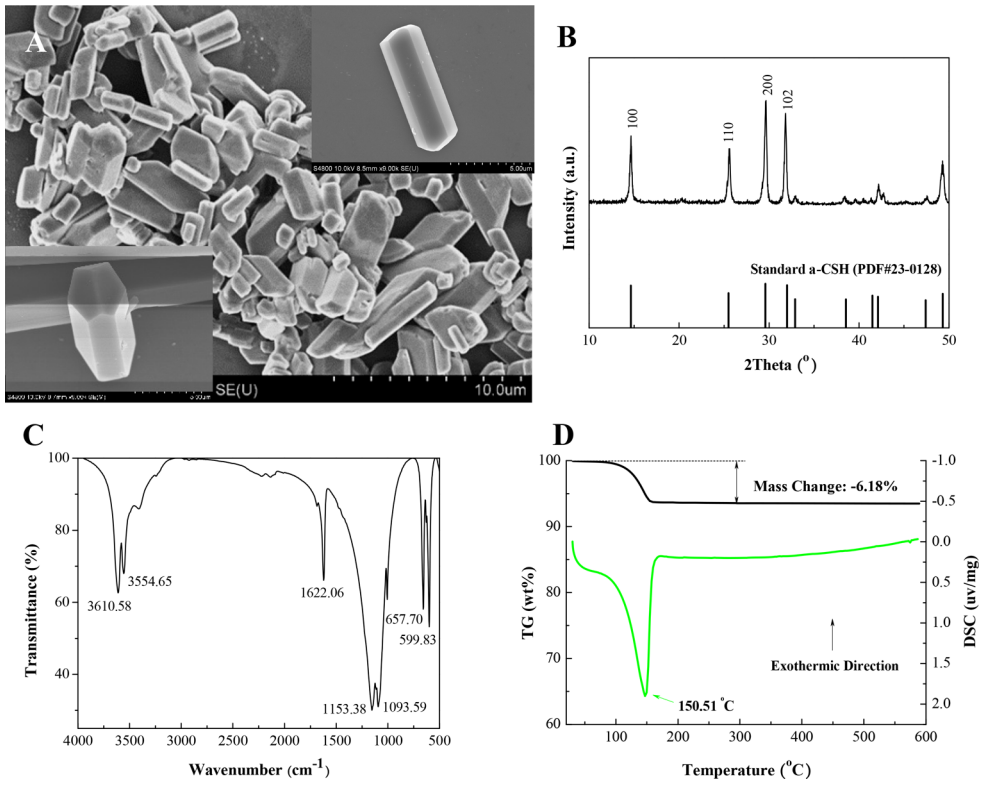

Figure 5. (A) SEM images, (B) XRD pattern, (C) FTIR spectrum, and (D) TG-DSC curves of α-CSH product prepared under optimum conditions.

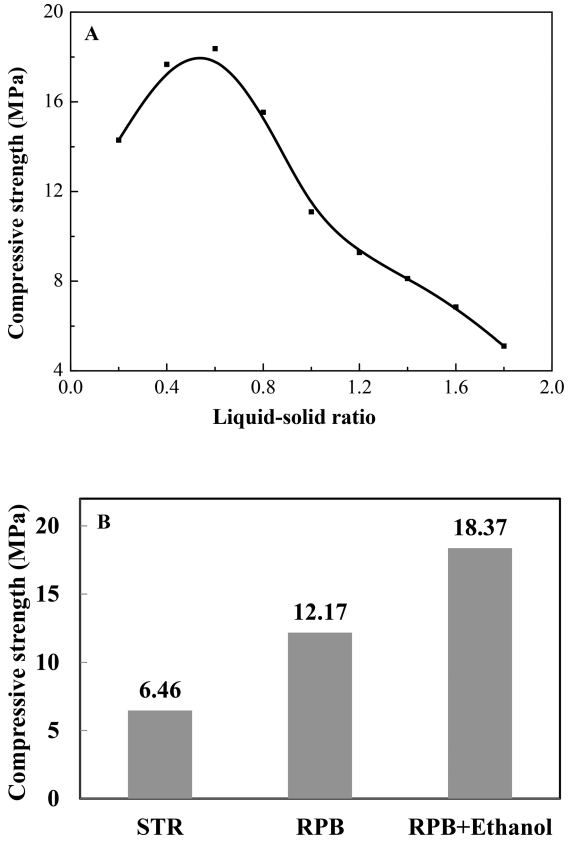

Figure 6. (A) Relationship between the liquid−solid ratio and the compressive strength of calcium sulfate bone material. (B) Compressive strengths of calcium sulfate bone materials prepared with different α-CSH samples.

because of the decreased size and lower aspect ratio. With the addition of ethanol in the RPB precipitation process, the compressive strength of the corresponding product was further increased by 50%, because of the smaller size and lower aspect ratio, reaching 18.37 MPa, which was much higher than that of non-load-bearing bone in the human body (5−8 MPa). It was concluded that the compressive strength of calcium sulfate bone material could be effectively adjusted by controlling the size and the shape of α-CSH crystals, according to different application requirements.

4. CONCLUSIONS

In this study, high-gravity reactive precipitation, combined with a salt solution method under atmospheric pressure, was first utilized to prepare α-CSH. The CSD precursor was facilely prepared via the reaction of Na_2SO_4 and $CaCl_2$, with the addition of ethanol as a morphology modifier, at an ethanol/water volume ratio of 1:3 in the RPB reactor. The $CaCl_2$ salt solution method at atmospheric pressure with 0.06 wt % citric acid additive was then adopted to dehydrate the as-prepared CSD precusor to obtain the final α-CSH product with a lower aspect ratio and smaller particle size. The results indicated that the RPB reactor had a greatly shortened precipitation time of CSD powders, from 30 min to 1 s, and the as-prepared CSD crystals had an obvious morphology change and significantly decreased size, in comparison to conventional STR. The size of CSD crystals could be further greatly reduced by properly adding ethanol. The final α-CSH crystals appeared as prism-shaped particles with a length of 1−6 μm, a width of 1−2 μm, and an aspect ratio of 1−3. Afterward, calcium sulfate bone materials were prepared by mixing α-CSH and normal saline at various liquid−solid ratios. With the increase of liquid−solid ratio, the compressive strength initially had an increase and

DOI: 10.1021/acs.iecr.7b03356
Ind. Eng. Chem. Res. 2017, 56, 14053−14059

then a subsequent decrease, reaching a maximum value of 18.37 MPa at a liquid−solid ratio of 0.6. The compressive strengths of the products from the RPB without and with ethanol were almost two and three times greater than that of the counterpart from the STR without ethanol. This study will provide a new route to the facile preparation of high-quality α-CSH for bone regeneration materials.

■ ASSOCIATED CONTENT

Supporting Information

The Supporting Information is available free of charge on the ACS Publications website at DOI: 10.1021/acs.iecr.7b03356.

Particles sizes and aspect ratios of CSD precursors prepared with no addition of ethanol in the STR and in the RPB reactor with different ethanol/water volume ratios (Table S1); photographs of the as-prepared calcium sulfate bone materials, and calcium sulfate bone material immersed in normal saline for 60 d (Figure S1) (PDF)

■ AUTHOR INFORMATION

Corresponding Authors

*Tel.: +86-10-64443134. Fax: +86-10-64444784. E-mail: zhll@mail.buct.edu.cn (L.-L. Zhang).

*Tel.: +86-10-64449453. Fax: +86-10-64423474. E-mail: wangjx@mail.buct.edu.cn (J.-X. Wang).

ORCID

Dan Wang: 0000-0002-3515-4590

Jie-Xin Wang: 0000-0003-0459-1621

Notes

The authors declare no competing financial interest.

■ ACKNOWLEDGMENTS

This work was financially supported by National Key Research and Development Program of China (No. 2016YFA0201701/2016YFA0201700), National Natural Science Foundation of China (Nos. 21622601 and 21576022), National Key Basic Research Program of China (No. 2015CB932100), and Guangdong Provincial Applied Science and Technology Research and Development Project (No. 2015B090927001).

■ REFERENCES

(1) Yang, J. C.; Wu, H. D.; Teng, N. C.; Ji, D. Y.; Lee, S. Y. Novel attempts for the synthesis of calcium sulfate hydrates in calcium chloride solutions under atmospheric conditions. *Ceram. Int.* **2012**, *38*, 381−387.

(2) Gitelis, S.; Piasecki, P.; Turner, T.; Haggard, W.; Charters, J. Use of a calcium sulfate-based bone graft substitute for benign bone lesions. *Orthopedics* **2001**, *24*, 162−166.

(3) Pan, Z. Y.; Lou, Y.; Yang, G. Y.; Ni, X.; Chen, M. C.; Xu, H. Z.; Miao, Xi. G.; Liu, J. L.; Hu, C. F.; Huang, Q. Preparation of calcium sulfate dihydrate and calcium sulfate hemihydrate with controllable crystal morphology by using ethanol additive. *Ceram. Int.* **2013**, *39*, 5495−5502.

(4) Woo, K. M.; Yu, B.; Jung, H. M.; Lee, Y. K. Comparative evaluation of different crystal-structured calcium sulfates as bone-filling materials. *J. Biomed. Mater. Res., Part B* **2009**, *91B*, 545−554.

(5) Jung, H. M.; Song, G. A.; Lee, Y. K.; Baek, J. H.; Ryoo, H. M.; Kim, G. S.; Choung, P. H.; Woo, K. M. Modulation of the resorptionand osteoconductivity of α-calcium sulfate by histone deacetylase inhibitors. *Biomaterials* **2010**, *31*, 29−37.

(6) Park, Y.; Dziak, R.; Genco, R.; Swihart, M.; Perinpanayagam, H. Calcium sulfate based nanoparticles. U.S. Patent No. 7767226B2, 2010.

(7) Wang, P.; Lee, E.; Park, C.; Yoon, B.; Shin, D.; Kim, H.; Koh, Y.-H.; Park, S.-H. Calcium sulfate hemihydrate powders with a controlled morphology for use as bone cement. *J. Am. Ceram. Soc.* **2008**, *91*, 2039−2042.

(8) Kong, B.; Guan, B. H.; Yates, M. Z.; Wu, Z. B. Control of α-calcium sulfate hemihydrate morphology using reverse micro-emulsions. *Langmuir* **2012**, *28*, 14137−14142.

(9) Guan, B. H.; Yang, L.; Fu, H. L.; Kong, B.; Li, T. Y.; Yang, L. C. α-Calcium sulfate hemihydrate preparation from FGD gypsum in recycling mixed salt solutions. *Chem. Eng. J.* **2011**, *174*, 296−303.

(10) Guan, B. H.; Yang, L. C.; Wu, Z. B.; Shen, Z. X.; Ma, X. F.; Ye, Q. Q. Preparation of α-calcium sulfate hemihydrate from FGD gypsum in K, Mg-containing concentrated $CaCl_2$ solution under mild conditions. *Fuel* **2009**, *88*, 1286−1293.

(11) Guan, B. H.; Fu, H. L.; Yu, J.; Jiang, G. M.; Kong, B.; Wu, Z. B. Direct transformation of calcium sulfite to α-calcium sulfate hemihydrate in a concentrated Ca-Mg-Mn chloride solution under atmospheric pressure. *Fuel* **2011**, *90*, 36−41.

(12) Kong, B.; Yu, J.; Savino, K.; Zhu, Y. G.; Guan, B. H. Synthesis of α-calcium sulfate hemihydrate submicron-rods in water/n-hexanol/CATB reverse microemulsion. *Colloids Surf., A* **2012**, *409*, 88−93.

(13) Hazra, C.; Bari, S.; Kundu, D.; Chaudhari, A.; Mishra, S.; Chatterjee, A. Ultrasound-assisted/biosurfactant-templated size-tunable synthesis of nano-calcium sulfate with controllable crystal morphology. *Ultrason. Sonochem.* **2014**, *21*, 1117−1131.

(14) Li, L.; Zhu, Y.; Ma, M. G Microwave-assisted preparation of calcium sulfate nanowires. *Mater. Lett.* **2008**, *62*, 4552−4554.

(15) Ling, Y.; Demopoulos, G. P. Preparation of α-calcium sulfate hemihydrate by reaction of sulfuric acid with lime. *Ind. Eng. Chem. Res.* **2005**, *44*, 715−724.

(16) Feldmann, T.; Demopoulos, G. P. The crystal growth kinetics of alpha calcium sulfate hemihydrate in concentrated $CaCl_2$-HCl solutions. *J. Cryst. Growth* **2012**, *351*, 9−18.

(17) Guan, B. H.; Yang, L. C.; Wu, Z. B. Effect of Mg^{2+} ions on the nucleation kinetics of calcium sulfate in concentrated calcium chloride solutions. *Ind. Eng. Chem. Res.* **2010**, *49*, 5569−5574.

(18) Liu, C.; Zhao, Q.; Wang, Y.; Shi, P.; Jiang, M. Hydrothermal synthesis of calcium sulfate whisker from flue gas desulfurization gypsum. *Chin. J. Chem. Eng.* **2016**, *24*, 1552−1560.

(19) Chen, J. M.; Gao, J.; Yin, H. B.; Liu, F. G.; Wang, A. L.; Zhu, Y. Q.; Wu, Z. A.; Jiang, T. S.; Qin, D. M.; Chen, B. J.; Ji, Y. Q.; Sun, M. Size-controlled preparation of α-calcium sulfate hemihydrate starting from calcium sulfate dihydrate in the presence of modifiers and the dissolution rate in simulated body fluid. *Mater. Sci. Eng., C* **2013**, *33*, 3256−3262.

(20) Tang, M. L.; Shen, X. D.; Huang, H. Influence of α-calcium sulfate hemihydrate particle characteristics on the performance of calcium sulfate-based medical materials. *Mater. Sci. Eng., C* **2010**, *30*, 1107−1111.

(21) Guo, K.; Zhang, Z.; Luo, H.; Dang, J.; Qian, Z. An innovative approach of the effective mass transfer area in the rotating packed bed. *Ind. Eng. Chem. Res.* **2014**, *53*, 4052−4058.

(22) Chen, J. F.; Wang, Y. H.; Guo, F.; Wang, X. M.; Zheng, C. Synthesis of nanoparticles with novel technology: high-gravity reactiveprecipitation. *Ind. Eng. Chem. Res.* **2000**, *39*, 948−954.

(23) Rao, D. P.; Bhowal, A.; Goswami, P. S. Process intensification in rotating packed beds (HIGEE): an appraisal. *Ind. Eng. Chem. Res.* **2004**, *43*, 1150−1162.

(24) Chen, J. F.; Shao, L.; Guo, F.; Wang, X. M. Synthesis of nanofibers of aluminum hydroxide in novel rotating packed bed reactor. *Chem. Eng. Sci.* **2003**, *58*, 569−575.

(25) Sun, Q.; Chen, B.; Wu, X.; Wang, M.; Zhang, C.; Zeng, X. F.; Wang, J. X.; Chen, J. F. Preparation of transparent suspension of lamellar magnesium hydroxide nanocrystals using a high-gravity reactive precipitation combined with surface modification. *Ind. Eng. Chem. Res.* **2015**, *54*, 666−671.

(26) Lv, B. Y.; Zhao, L. S.; Pu, Y.; Le, Y.; Zeng, X. F.; Chen, J. F.; Wen, N.; Wang, J. X. Facile preparation of controllable-aspect-ratio hydroxyapatite nanorods with high-hravity technology for bone tissue engineering. *Ind. Eng. Chem. Res.* **2017**, *56*, 2976−2983.
(27) Yang, Q.; Wang, J. X.; Guo, F.; Chen, J. F. Preparation of hydroxyaptite nanoparticles by using high-gravity reactive precipitation combined with hydrothermal method. *Ind. Eng. Chem. Res.* **2010**, *49*, 9857−9863.
(28) Zhao, H.; Wang, J. X.; Zhang, H. X.; Shen, Z. G.; Yun, J.; Chen, J. F. Facile preparation of hydrophobic pharmaceutical danazol nanoparticles by high-gravity anti-solvent precipitation (HGAP) method. *Chin. J. Chem. Eng.* **2009**, *17*, 318−323.
(29) Chen, J. F.; Zhang, J. Y.; Shen, Z. G.; Zhong, J.; Yun, J. Preparation and characterization of amorphous cefuroxime axetil drug nanoparticles with novel technology: high-gravity antisolvent precipitation. *Ind. Eng. Chem. Res.* **2006**, *45*, 8723−8727.
(30) Guo, K.; Guo, F.; Feng, Y. D.; Chen, J. F.; Zheng, C.; Gardner, N. C. Synchronous visual and RTD study on liquid flow in rotatingpacked bed contactor. *Chem. Eng. Sci.* **2000**, *55*, 1699−1706.
(31) Feldmann, T.; Demopoulos, G. P. Effects of crystal habit modifiers on the morphology of calcium sulfate dehydrate grown in strong $CaCl_2$−HCl solutions. *J. Chem. Technol. Biotechnol.* **2014**, *89*, 1523−1533.
(32) Mao, X. L.; Song, X. F.; Lu, G. M.; Xu, Y. X.; Sun, Y. Z.; Yu, J. G. Effect of additives on the morphology of calcium sulfate hemihydrate: Experimental and molecular dynamics simulation studies. *Chem. Eng. J.* **2015**, *278*, 320−327.
(33) Li, F.; Liu, J. L.; Yang, G. Y.; Pan, Z. Y.; Ni, X.; Xu, H. Z.; Huang, Q. Effect of pH and succinic acid on the morphology of α-calcium sulfate hemihydrate synthesized by a salt solution method. *J. Cryst. Growth* **2013**, *374*, 31−36.

DOI: 10.1021/acs.iecr.7b03356
Ind. Eng. Chem. Res. 2017, 56, 14053−14059